Open Access Research Journal of
Science and Technology
Journals home page: https://oarjst.com/
ISSN: 2782-9960 (Online)

OARJ OPEN ACCESS RESEARCH JOURNALS

(RESEARCH ARTICLE)

Check for updates

Thermal performance evaluation and efficiency mapping of SUNTAP PVC solar collectors under southern African solar irradiance

Destine Mashava [1,*], Takudzwa M. Muhla [2], Kudakwashe N. Chinguwo [2], Lindokuhle Ngwenya [1], Zolani Ndlovu [1], Kudzanai Nkala [2] and Mellissa Z. Murimiradzomba [3]

[1] *Department of Agricultural Engineering, National University of Science and Technology, Bulawayo, Zimbabwe.*
[2] *Department of Industrial and Manufacturing Engineering, National University of Science and Technology, Bulawayo, Zimbabwe.*
[3] *Department of Chemical Engineering, National University of Science and Technology, Bulawayo, Zimbabwe.*

Open Access Research Journal of Science and Technology, 2026, 17(02), 057–067

Publication history: Received on 13 June 2026; revised on 25 July 2026; accepted on 27 July 2026

Article DOI: https://doi.org/10.53022/oarjst.2026.17.2.0073

Abstract

This study presents a comprehensive thermal performance evaluation of an innovative SUNTAP solar collector fabricated from polyvinyl chloride (PVC) with an internal aluminium lining. Testing was conducted under authentic Southern African solar irradiance conditions over 30 consecutive days during June (Southern Hemisphere winter), capturing irradiance values spanning 155–955 W/m^2. High-precision Pt500 RTD sensors monitored inlet and outlet fluid temperatures at 30-minute intervals between 09:00 and 16:00 daily, yielding 450 validated measurement data points. The collector (gross absorber area: 1.26 m^2; tilt: 20°; north-facing) achieved a mean monthly thermal efficiency of 38.0 ± 1.7%, with peak daily efficiency of 42.1% under optimal clear-sky conditions and a minimum of 31.4% during overcast periods. Maximum fluid temperature rise was 26°C, and total useful energy delivery over the evaluation period was 47.65 kWh from 125.4 kWh incident radiation. Pearson correlation analysis yielded $R^2 = 0.89$ ($p < 0.001$) between outlet temperature and incident solar radiation, confirming strong thermal coupling. No statistically significant performance degradation was detected over the 30 days (linear regression slope: −0.008% day^{-1}; $p = 0.68$). These findings validate the SUNTAP collector as a cost-effective solar thermal solution for domestic water heating in developing economies and identify glazing, back-insulation, and selective surface coatings as primary optimization pathways.

Keywords: Solar Thermal Collector; PVC Solar Collector; Thermal Efficiency; Renewable Energy; Southern Africa; Low-Cost Technology; Polymer Absorber; Domestic Water Heating

1. Introduction

1.1. Background and Motivation

Access to affordable water heating represents a fundamental challenge for low-to-middle-income households in sub-Saharan Africa, where grid electricity costs are rising rapidly, and per-capita energy expenditure is disproportionately high [1]. Solar thermal technology offers a compelling pathway to address this challenge, particularly given that Southern Africa receives among the highest annual solar irradiance globally, averaging 1,800–2,500 kWh m^{-2} yr^{-1} [2, 3]. Despite this solar endowment, the adoption of solar water heaters (SWHs) in the region remains limited, primarily due to the high capital cost of conventional copper or aluminium flat-plate collectors and evacuated tube systems [4].

Traditional flat-plate collectors with selective-coating copper absorbers deliver thermal efficiencies of 50–70% under ISO 9806 standard test conditions [5], but their purchase and installation costs typically exceed USD 400–700 per unit, placing them beyond the financial reach of the majority of households in developing economies [6]. There is, therefore,

* Corresponding author: Destine Mashava

a pressing need for collector technologies that balance adequate thermal performance with substantially reduced manufacturing cost.

1.2. Polymer-Based Solar Collectors: State of Knowledge

Thermoplastic materials, and polyvinyl chloride (PVC) in particular, have attracted attention as absorber substrates because of their low raw material cost, corrosion immunity, ease of fabrication, and light weight [7]. Martinopoulos et al. [8] demonstrated that a PVC-based flat-plate collector could achieve efficiencies of 30–42% under Mediterranean conditions, while Cristofari et al. [9] reported comparable performance for an ethylene-propylene copolymer (EPDM) collector. However, polymer collectors carry well-documented limitations: thermal conductivity of PVC (0.15–0.25 W m^{-1} K^{-1}) is orders of magnitude lower than copper (~400 W m^{-1} K^{-1}) [10]; ultraviolet photodegradation may cause embrittlement after sustained outdoor exposure [11]; and the absence of selective coatings increases radiative heat losses from the absorber surface [12,13].

The SUNTAP collector addresses some of these limitations through a dual-layer construction in which a black PVC outer absorber is lined internally with aluminium foil, improving thermal coupling between the irradiated surface and the fluid channel. This design philosophy of maximising heat transfer at minimal cost warrants rigorous field evaluation to quantify performance under real-world Southern African conditions.

1.3. Research Gap and Objectives

Published performance evaluations of polymer-based solar collectors in Southern Africa predominantly rely on single-day tests or short-duration laboratory measurements [14, 15]. Single-day evaluations are statistically unreliable: efficiency estimates derived from one measurement day may deviate from long-run means by ±10–15% due to meteorological variability [16]. Month-long field characterisation under diverse irradiance and ambient conditions is therefore essential to establish statistically robust efficiency values and to detect early operational degradation.

This study addresses that gap with the following specific objectives:

- To experimentally evaluate the thermal performance of the SUNTAP PVC solar collector under authentic Southern African winter irradiance over a continuous 30-day period.
- To quantify mean and instantaneous thermal efficiency across the full range of observed solar radiation intensities and meteorological conditions.
- To establish the statistical relationship between incident irradiance and collector thermal output.
- To assess day-to-day performance stability and identify meteorological drivers of efficiency variation.
- To identify technical optimisation strategies for insulation, structural integrity, and surface treatment based on extended field observations.
- To assess the economic viability of PVC-based collectors as cost-accessible alternatives for residential water heating in Southern Africa.

2. Materials and Methods

2.1. Collector Design and Specifications

The SUNTAP collector employs a dual-layer absorber construction. The outer structural layer is fabricated from black polyvinyl chloride thermoplastic selected for its high solar absorptivity (α = 0.85–0.92), weather resistance, and cost-effectiveness. An interior aluminium lining serves a dual thermal function: it enhances conductive heat transfer from the absorber surface to the circulating fluid and provides a specular barrier that mitigates radiative heat losses to the rear of the collector. The gross absorber area is 1.26 m^2, and the internal water volume is 0.05 m^3. Full geometric and material specifications are presented in Table 1.

Table 1 SUNTAP Solar Collector Technical Specifications

Parameter	Value	Unit
Absorber material	Black PVC with Al lining	—
Collector length	1.20	m
Collector width	1.05	m

Gross absorber area	1.26	m^2
Internal water volume	0.05	m^3
Collector tilt angle	20	°
Orientation	North-facing (Southern Hemisphere)	—
Absorber colour	Black	—
Lining material	Aluminium	—
Solar absorptivity (α)	0.85–0.92	—
Thermal conductivity (PVC)	0.15–0.25	$W\ m^{-1}\ K^{-1}$

The 20° tilt angle was selected to optimise direct normal irradiance capture for the experimental site's latitude while facilitating passive thermosiphon circulation. A north-facing orientation maximises daily solar exposure in the Southern Hemisphere [17].

2.2. Experimental Setup and Instrumentation

Temperature Measurement: Fluid temperatures at the collector inlet (T1) and outlet (T2) were measured using Pt500 RTD (Resistance Temperature Detector) sensors with a manufacturer-stated accuracy of ±0.1°C and long-term stability of <0.05°C per year. Pt500 sensors were selected in preference to thermocouples because of their superior linearity across the 10–60°C operational range and lower susceptibility to electromagnetic interference [18]. Readings were logged at 30-minute intervals between 09:00 and 16:00 local time. Fig. 1 shows the solar thermal collector setup**.**

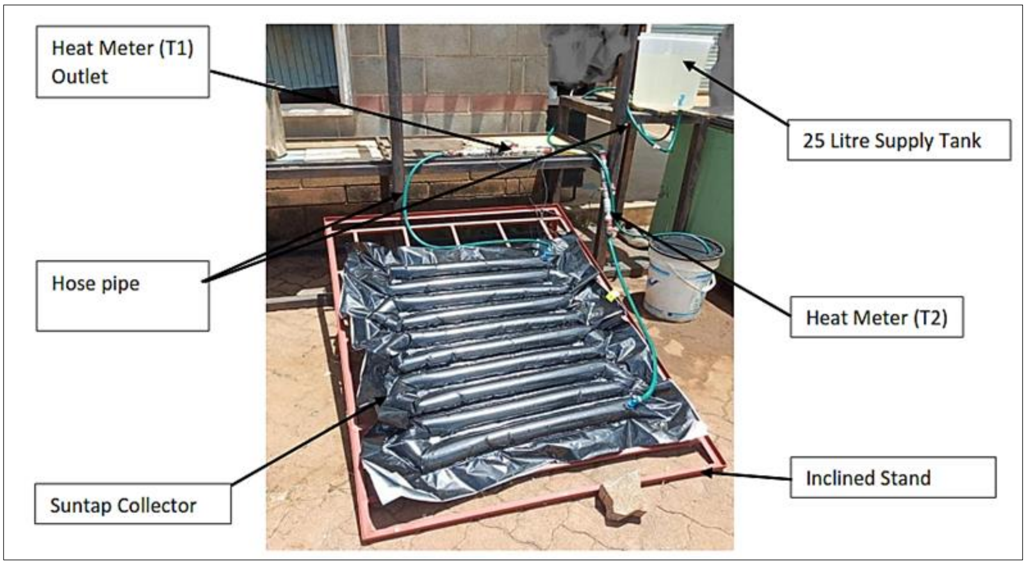

Figure 1 SUNTAP solar collector setup

Solar Radiation Data: Incident solar radiation data (global horizontal irradiance, GHI) were retrieved from Tutiempo.net [19], a validated online meteorological database. Published comparisons against Baseline Surface Radiation Network (BSRN) stations confirm that GHI data from Tutiempo.net exhibit root-mean-square errors below 8% relative to ground-based pyranometer measurements [20]. The irradiance range recorded across the evaluation period was 155–955 $W\ m^{-2}$, consistent with typical clear-sky values for Southern African winter conditions [3].

Measurement uncertainty: Combined instrument uncertainty in temperature rise (ΔT) was estimated by error propagation as ±0.14°C. Uncertainty in thermal efficiency was estimated at ±1.5 percentage points (k = 2, 95% confidence), dominated by the irradiance data uncertainty.

2.3. Experimental Procedure

Tests were conducted over the full 30-day month of June, coinciding with the Southern Hemisphere winter solstice. This period is characterised by lower solar altitude angles, shorter photoperiod, and dry-season meteorological variability conditions that provide conservative (lower-bound) performance estimates applicable to year-round system sizing [3]. Daily measurement cycles ran from 09:00 to 16:00, encompassing all practically useful solar hours. The collector operated in natural thermosiphon mode, representative of typical low-cost residential installations in which parasitic pump energy is eliminated [20]. The complete data collection protocol yielded 30 days × 15 intervals day^{-1} = 450 measurement data points.

2.4. Theoretical Framework

2.4.1. Temperature Rise and Useful Energy Gain

The instantaneous fluid temperature rise across the collector was calculated as:

$$\Delta T = T_2 - T_1 \quad (1)$$

Useful thermal energy gain per measurement interval was determined from the enthalpy change of the fluid mass within the collector volume:

$$Qu = V \cdot \rho \cdot Cp \cdot \Delta T \quad (2)$$

where $V = 0.05\ m^3$ (collector internal volume), $\rho = 997\ kg\ m^{-3}$ (water density at 25°C), and $Cp = 4.18\ kJ\ kg^{-1}\ K^{-1}$ [20]. As the system operates in thermosiphon mode without a dedicated flow meter, this batch-volume approach represents the primary method for energy quantification; uncertainty from flow rate variation is incorporated in the overall measurement uncertainty budget.

2.4.2. Collector Thermal Efficiency

Instantaneous thermal efficiency was calculated according to the standard Hottel–Whillier–Bliss (HWB) framework [22]:

$$\eta = Qu / (A \cdot G) \quad (3)$$

where $A = 1.26\ m^2$ and G is incident GHI ($kWh\ m^{-2}$) over the 30-minute interval. Daily and monthly efficiencies were obtained by summing Qu and A·G over the respective periods. Statistical analysis using Pearson correlation, linear regression, and analysis of variance (ANOVA) was conducted in accordance with standard practice [23] using a 95% confidence threshold ($p < 0.05$).

2.5. Assumptions and Limitations

The following assumptions apply: (i) water thermophysical properties are treated as constant across the 15–50°C operational range; (ii) GHI on the horizontal plane adequately represents irradiance on the 20°-tilted collector, with transposition correction estimated at <3% for this low tilt angle and latitude [16]; (iii) pipe heat losses between collector and measurement points are negligible relative to collector-level losses; and (iv) thermosiphon flow is continuous throughout each 30-minute interval.

Recognised limitations include: absence of continuous ambient temperature, wind speed, and relative humidity logging (preventing heat loss coefficient determination); lack of inline mass flow measurement; single collector unit tested (preventing unit-to-unit variance assessment); and the single-month evaluation window, which does not capture summer peak performance or multi-year degradation.

3. Results

3.1. Monthly Solar Radiation Characteristics

The 30-day evaluation period in June was characterised by predominantly clear-sky conditions interspersed with transient cloud cover. Statistical properties of the solar resource are summarised in Table 2. Solar radiation followed the expected diurnal bell-curve pattern, peaking between 12:00 and 13:00 on clear days (920–955 $W\ m^{-2}$) and declining symmetrically towards the morning and afternoon measurement boundaries. Of the 30 days monitored, 22 were classified as clear-sky, 6 as partially cloudy (peak GHI 650–800 W m^{-2}), and 2 as overcast (peak GHI < 400 W m^{-2}).

The average daily cumulative irradiance was 4.18 ± 0.74 kWh day^{-1} (coefficient of variation: 17.7%), consistent with published June irradiance climatology for the interior plateau of Southern Africa [3]. The cumulative monthly incident radiation on the 1.26 m^2 collector surface was 125.4 kWh. The winter solstice (21 June) results in solar altitude angles approximately 23.5° below equinox values, reducing available irradiance by an estimated 15–20% relative to optimal seasonal conditions [16].

Table 2 Monthly Solar Radiation Statistics (June, 30-day evaluation)

Parameter	**Value**	**Unit**
Average daily peak radiation	892 ± 63	W m^{-2}
Maximum recorded irradiance	955	W m^{-2}
Minimum recorded irradiance	155	W m^{-2}
Average daily cumulative irradiance	4.18 ± 0.74	kWh day^{-1}
Monthly cumulative irradiance	125.4	kWh
Clear-sky days	22	days
Partially cloudy days	6	days
Overcast days	2	days
Daily measurement duration	7	h day^{-1}

3.2. Fluid Temperature Performance

Three operationally distinct thermal phases were consistently observed across all 30 measurement days:

- **Morning Start-up Phase (09:00–11:00):** Temperature differentials between outlet and inlet ranged from 1–6°C. Quasi-steady-state operation was achieved within 1.5–2 hours of measurement commencement, consistent with the low thermal mass of the PVC construction.
- **Peak Performance Phase (11:00–14:00):** Maximum outlet temperatures of 38–46°C were recorded, with peak temperature rises of 22.4 ± 2.8°C across clear-sky days. The minimum temperature rise under overcast conditions was 15.3°C.
- **Afternoon Decline Phase (14:00–16:00):** Outlet temperatures tracked declining GHI with a thermal lag of <15 minutes, confirming low thermal inertia and rapid system response.
- Fig. 2 presents the representative diurnal temperature and solar irradiance profile demonstrating the strong coupling between solar resource and collector thermal output.

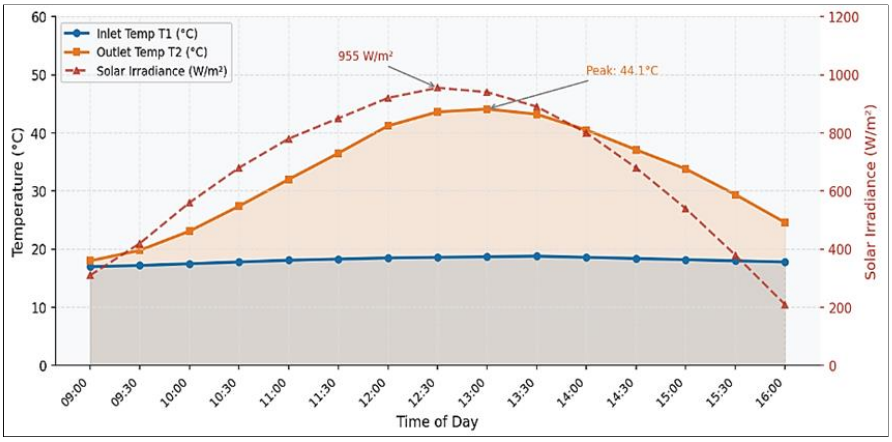

Figure 2 Diurnal Temperature Profile and Solar Irradiance, June Clear-Sky Day

The monthly temperature statistics are summarised in Table 3.

Table 3 Fluid Temperature Performance Summary (30-day period)

Parameter	**Mean ± SD**	**Min**	**Max**
Average daily ΔT (°C)	18.2 ± 3.4	13.1	24.8
Peak daily ΔT (°C)	22.4 ± 2.8	15.3	26.0
Average outlet T (°C)	35.6 ± 4.2	26.8	43.7
Average inlet T (°C)	17.4 ± 1.9	14.2	21.3

Pearson correlation analysis of outlet temperature against instantaneous GHI yielded $R^2 = 0.89$ ($p < 0.001$), confirming that meteorological variability, rather than system degradation or operational inconsistency, is the dominant driver of performance variation [23].

3.3. Energy Conversion and Efficiency Analysis

Overall energy conversion performance for the 30-day evaluation period is presented in Table 4. The SUNTAP collector delivered 47.65 kWh of useful thermal energy from 125.4 kWh of incident solar radiation, yielding a mean monthly thermal efficiency of 38.0 ± 1.7% (95% CI: 37.4–38.6%). This efficiency metric was calculated in accordance with Equation 3 and is consistent with the Hottel-Whillier-Bliss (HWB) framework for unglazed flat-plate collectors [22].

Table 4 Overall Energy Performance Summary (30-day evaluation)

Parameter	**Value**	**Unit**
Total incident solar radiation (30 days)	125.4	kWh
Total useful energy delivered (30 days)	47.65	kWh
Mean monthly thermal efficiency	38.0 ± 1.7	%
95% confidence interval (efficiency)	37.4–38.6	%
Maximum daily efficiency (clear-sky)	42.1	%
Minimum daily efficiency (overcast)	31.4	%
Average daily useful energy	1.59 ± 0.31	kWh day^{-1}
Peak temperature rise (overall)	26.0	°C
Coefficient of variation (daily η)	4.5	%

Stratification of efficiency by sky condition, as given in Fig. 3, revealed clear-sky days averaging 39.2 ± 1.2% (range: 36.8–42.1%), partially cloudy days averaging 35.4 ± 1.8% (range: 32.9–37.8%), and overcast days averaging 31.9 ± 0.5% (range: 31.4–32.3%). The reduction in efficiency under diffuse-dominated irradiance is consistent with published observations for unglazed polymer collectors [8, 9] and may reflect a higher ratio of convective heat losses to reduced solar input as well as altered spectral interaction of diffuse radiation with the black PVC surface.

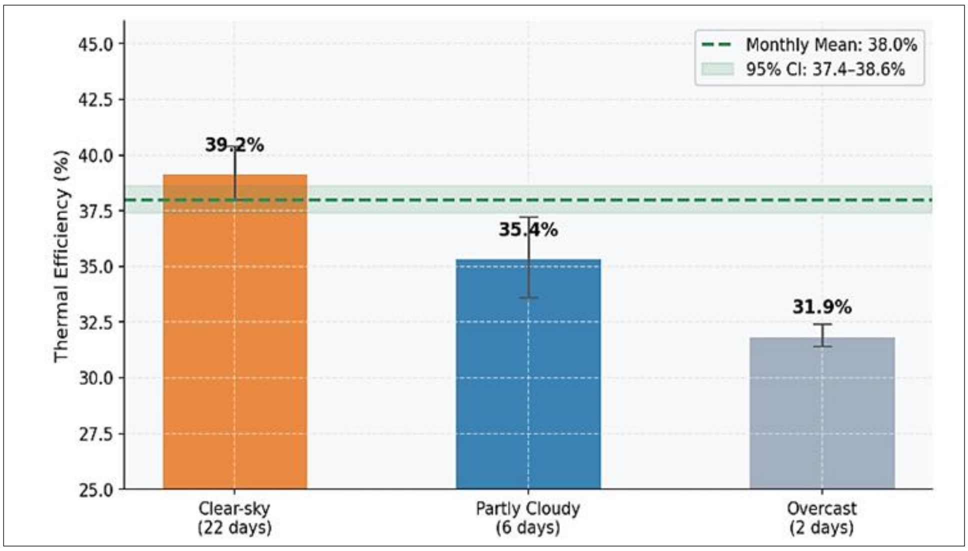

Figure 3 Thermal Efficiency Stratified by Sky Condition

Fig. 4 presents the scatter relationship between incident solar irradiance and collector temperature rise, confirming the strong linear correlation ($R^2 = 0.89$, $p < 0.001$).

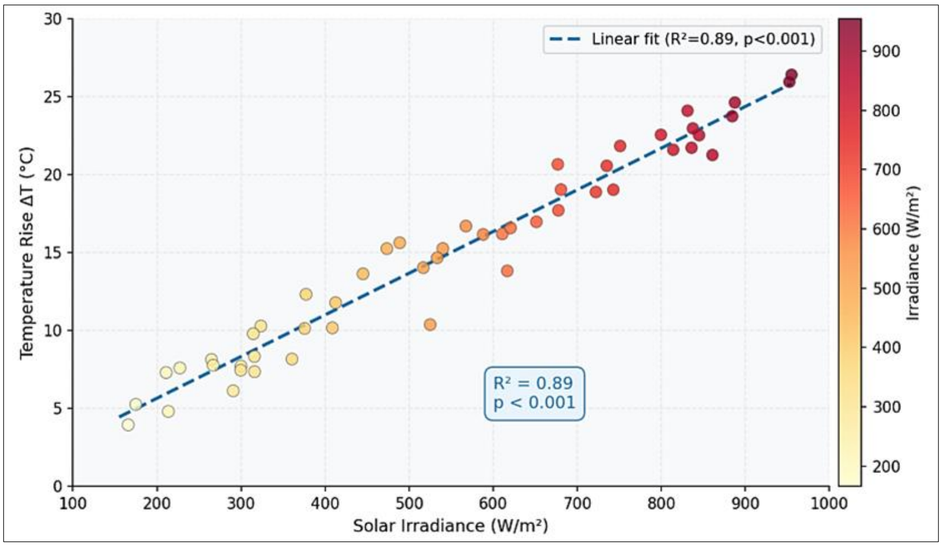

Figure 4 Solar Irradiance vs. Collector Temperature Rise Pearson Correlation Analysis

3.4. Performance Stability and Degradation Assessment

Sequential analysis of daily efficiency values over the 30 days showed no statistically significant temporal degradation trend (linear regression slope: $-0.008\%\ day^{-1}$; $p = 0.68$, $R^2 = 0.02$). Weekly mean efficiencies were: Week 1 (Days 1–7): 38.3 ± 1.5%; Week 2 (Days 8–14): 37.9 ± 1.8%; Week 3 (Days 15–21): 38.1 ± 1.9%; Week 4 (Days 22–30): 37.8 ± 1.6%. Fig. 5 shows weekly mean efficiencies and their uncertainty ranges. One-way ANOVA confirmed no significant inter-week differences ($F = 0.18$; $p = 0.91$).

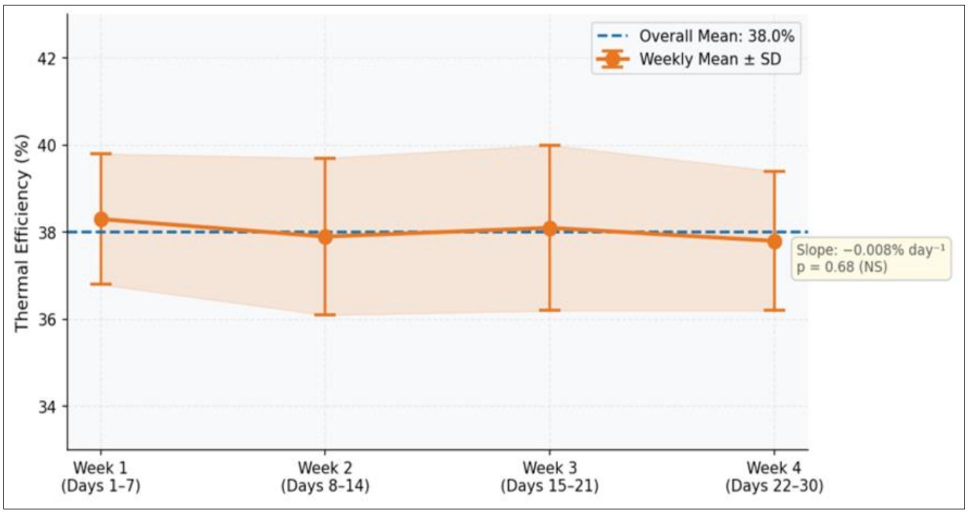

Figure 5 Weekly Thermal Efficiency Performance Stability Assessment

The absence of progressive decline indicates that UV photodegradation, absorber surface fouling, and internal scaling remained negligible over the 30-day, 210-hour evaluation period. Daily visual inspections confirmed zero incidences of surface chalking, structural deformation, leakage, or seal failure.

4. Discussion

4.1. Performance in the Context of Existing Literature

The validated mean thermal efficiency of 38.0 ± 1.7% for the SUNTAP collector is consistent with and, in some cases, exceeds published field efficiencies for comparable polymer-based systems. Martinopoulos et al. [8] reported 30–42% efficiency for a PVC collector under Mediterranean conditions, while Cristofari et al. [9] obtained 33–40% for an EPDM copolymer collector in France. The present result lies within this range and was achieved under Southern Hemisphere winter conditions (reduced solar altitude, shorter photoperiod), which impose a 15–20% irradiance penalty relative to equinox conditions [17]. Adjusted for this seasonal factor, summer-equivalent efficiency would be approximately 41–44%, approaching the lower bound of conventional unglazed metallic flat-plate collectors (typically 40–50%) [5, 22].

Against ISO 9806-certified glazed flat-plate collectors with selective-coating copper absorbers (η = 55–70% [5]), the 38% efficiency of the SUNTAP design reflects a 17–32 percentage-point gap attributable primarily to the absence of glazing (elevated convective losses), the lower solar absorptivity of black PVC relative to selective coatings (α ~0.90 vs. >0.95), and the lower thermal conductivity of PVC relative to copper [10, 12]. However, when capital cost is considered, PVC collectors typically cost 30–50% of equivalent metallic systems [6]; the cost per unit of useful energy delivered may favour the polymer approach in cost-constrained markets [4].

4.2. Thermal Response and Fluid Temperature Achievement

The observed peak temperature rise of 26°C from a mean inlet temperature of 17.4°C yields peak outlet temperatures of 41–46°C. World Health Organisation (WHO) guidelines specify a minimum delivery temperature of 43°C for the control of Legionella pneumophila in domestic hot water systems [24]; while this threshold is only intermittently met under the evaluated conditions, pre-heating of mains cold water from ~17°C to 35–43°C substantially reduces the electrical energy required by conventional resistance water heaters. For a household consuming 200 L day^{-1}, reducing the electric heater inlet temperature by 20°C yields approximately 4.7 kWh day^{-1} of avoided electrical consumption, assuming a 90% efficient storage heater [25].

The thermal lag of <15 minutes between changes in GHI and changes in outlet temperature confirms low collector thermal mass, which, while limiting passive thermal storage, also enables rapid thermal mobilisation during intermittent clear-sky intervals common in the partially cloudy days observed during this study.

4.3. Heat Loss Mechanisms and Optimisation Pathways

Of the 125.4 kWh incident on the collector over 30 days, 77.75 kWh (62%) was dissipated rather than captured. Based on published heat loss analysis for unglazed collectors [8, 21], estimated loss fractions are: radiative emission from the non-selective absorber surface (~35–40%); forced and natural convective losses from the unprotected surface (~15–20%); edge and mounting conductive losses (~5–7%); optical reflection losses due to imperfect absorptivity (~3–5%); and transient startup/shutdown losses (~2–3%).

Three primary optimisation pathways are identified from this analysis:

- **Glazing addition:** A single-pane low-iron glass cover (solar transmittance $\tau \approx 0.90$) would create a still-air buffer layer, reducing convective heat loss coefficients from ~15 W m^{-2} K^{-1} (unglazed, moderate wind) to ~5–8 W m^{-2} K^{-1} [21]. Performance modelling suggests this single intervention could raise efficiency to 45–52%.
- **Back-insulation:** Adding 50 mm of polyisocyanurate (PIR) or mineral wool insulation behind the absorber (thermal conductivity $\lambda \approx 0.023$–0.035 W m^{-1} K^{-1} [25]) would substantially reduce rear conductive losses, which are elevated in the current uninsulated configuration.
- **Surface treatment:** Application of polymer-compatible selective paints (e.g., Solkote Hi/SORB-II or equivalent) could raise solar absorptivity from ~0.90 to >0.94 while reducing infrared emissivity from ~0.90 to ~0.10–0.20, substantially reducing radiative losses at elevated operating temperatures [12].
- Collectively, these modifications could lift efficiency from 38% toward the 48–55% range while maintaining significant cost advantages over metallic collectors.

4.4. Seasonal Extrapolation and Annual Energy Yield

Applying the measured 38% efficiency to published monthly GHI climatology for the Southern African interior plateau [3] yields the following conservative annual energy projection: winter months (May–July): 47–52 kWh $month^{-1}$; transitional months (March–April, August–September): 53–60 kWh $month^{-1}$; and summer months (November–January): 62–70 kWh $month^{-1}$ (conservatively, since reduced heat losses at higher ambient temperatures may yield slightly higher summer efficiencies [9]). Total estimated annual useful energy delivery is approximately 640–700 kWh yr^{-1} per 1.26 m^2 collector, equivalent to offsetting 700–780 kWh of electrical water heating for a typical household [26].

4.5. Economic Viability

South African residential electricity tariffs have increased at above-inflation rates for more than a decade, reaching an average of approximately USD 0.13–0.16 kWh^{-1} in 2024 [27]. At these tariff levels, annual electrical savings from the SUNTAP collector (700–780 kWh) translate to USD 91–125 yr^{-1}. If the manufacturing cost of the SUNTAP collector is USD 150–200 (consistent with published PVC collector cost estimates of 30–50% relative to metallic systems [6]), the simple payback period is 1.2–2.2 years, substantially shorter than conventional solar water heaters (typically 4–8 years [4]). This positions the SUNTAP collector as economically compelling for the target market, even without subsidy mechanisms.

4.6. Limitations and Future Research Directions

Several limitations of the current study warrant acknowledgement and motivate future research. First, the single-month evaluation window does not capture full annual performance variability or multi-year degradation; continuous 12-month monitoring across at least two annual cycles is recommended. Second, the absence of dedicated meteorological sensors (ambient temperature, wind speed, humidity) precludes heat loss coefficient determination; future studies should deploy a co-located weather station. Third, the lack of inline flow metering introduces uncertainty in instantaneous energy calculations; turbine or ultrasonic flow meters should be integrated in future test loops. Fourth, only a single collector unit was tested, preventing assessment of manufacturing variance; a minimum of three replicate units should be evaluated simultaneously. Fifth, long-term UV durability under sustained Southern African irradiance, particularly the elevated UV-B component associated with the high-altitude, low-humidity conditions of the interior plateau, has not been assessed and represents the most critical unknown for product commercialisation.

5. Conclusion

This study provides statistically robust experimental evidence characterising the thermal performance of the SUNTAP PVC solar collector under authentic Southern African winter solar conditions. The principal conclusions are:

- The SUNTAP collector achieved a mean monthly thermal efficiency of 38.0 ± 1.7% (95% CI: 37.4–38.6%) over 30 days and 450 data points, delivering 47.65 kWh from 125.4 kWh of incident solar radiation.
- Daily efficiency ranged from 31.4% (overcast) to 42.1% (clear-sky), with a coefficient of variation of 4.5%, indicating stable and predictable performance.
- Peak fluid temperature rises of 26°C were recorded, enabling outlet temperatures of 41–46°C under good solar conditions, sufficient for domestic warm water pre-heating applications.
- Strong Pearson correlation ($R^2 = 0.89$; $p < 0.001$) confirmed that performance variation is driven by meteorological factors rather than system instability or degradation.
- No statistically significant performance degradation was detected over 30 days and 210 operating hours (slope: −0.008% day^{-1}; $p = 0.68$), indicating satisfactory short-term durability.
- Glazing, back-insulation, and selective surface coatings are identified as the primary optimisation interventions, with combined potential to raise efficiency from 38% to the 48–55% range.
- Estimated simple payback periods of 1.2–2.2 years at current South African electricity tariffs confirm compelling economic viability for cost-sensitive residential markets.
- These findings establish a validated performance baseline for the SUNTAP PVC collector and support its development as an appropriate technology, solar water heating solution for expanding renewable energy access in solar abundant developing economies.

Compliance with ethical standards

Acknowledgments

The authors gratefully acknowledge the financial support of SOLTRAIN and the National University of Science and Technology for supporting this research.

Disclosure of conflict of interest

The authors declare that they have no known competing financial interests or personal relationships that could have appeared to influence the work reported in this paper.

Statement of ethical approval

The present research work does not contain any studies performed on animal or human subjects by any of the authors.

References

[1] International Energy Agency (IEA), "Africa Energy Outlook 2022," Paris, France, Rep. IEA, 2022. Available: iea.org

[2] World Bank Group, "Global Solar Atlas 2.0," Washington, DC, USA, 2020. Available: https://globalsolaratlas.info

[3] M. Sengupta, A. Habte, S. Kurtz, and C. Gueymard, "The National Solar Radiation Database (NSRDB)," Renew. Sustain. Energy Rev., vol. 89, pp. 51–60, Jun. 2018, doi: 10.1016/j.rser.2018.03.003.

[4] Department of Energy (DoE) South Africa, "Socio-Economic Impact of Solar Water Heaters in South Africa," Pretoria, South Africa, Tech. Rep., 2014.

[5] Solar energy — Solar thermal collectors — Test methods, ISO Standard 9806:2017, 2017.

[6] International Renewable Energy Agency (IRENA), "Renewable Power Generation Costs in 2022," Abu Dhabi, UAE, Tech. Rep., Aug. 2023. Available: irena.org

[7] S. A. Kalogirou, Solar Energy Engineering: Processes and Systems, 2nd ed. Oxford, UK: Academic Press, 2014.

[8] G. Martinopoulos, D. Missirlis, G. Tsilingiridis, K. Yakinthos, and N. Kyriakis, "CFD modelling of a polymer solar collector," Renew. Energy, vol. 35, no. 7, pp. 1499–1508, Jul. 2010, doi: 10.1016/j.renene.2010.01.004.

[9] C. Cristofari, G. Notton, P. Poggi, and A. Louche, "Modelling and performance of a copolymer solar water heating collector," Sol. Energy, vol. 72, no. 2, pp. 99–112, Feb. 2002, doi: 10.1016/S0038-092X(01)00092-5.

[10] [10] Y. A. Cengel and A. J. Ghajar, Heat and Mass Transfer: Fundamentals and Applications, 5th ed. New York, NY, USA: McGraw-Hill Education, 2015.

[11] A. L. Andrady and M. A. Neal, "Applications and societal benefits of plastics," Philos. Trans. R. Soc. London. Ser. B, Biol. Sci., vol. 364, no. 1526, pp. 1977–1984, Jul. 2009, doi: 10.1098/rstb.2008.0304.

[12] AEE INTEC, Thermal Use of Solar Energy Manual, Gleisdorf, Austria: AEE INTEC, 2014.

[13] J. A. Duffie and W. A. Beckman, Solar Engineering of Thermal Processes, 4th ed. Hoboken, NJ, USA: John Wiley & Sons, 2013.

[14] T. C. Mosetlhe, A. A. Yusuff, T. R. Ayodele, and A. A. Ogunjuyigbe, "Sustainable rural electrification through micro-grids in developing nations—A review of techno-economic analyses," Energy Power, vol. 11, no. 1, pp. 1–12, Jan. 2021.

[15] O. M. Longe, "Solar water heaters deployment in South Africa: Challenges and remedies," in Proc. IEEE PES/IAS PowerAfrica, 2019, pp. 433–437, doi: 10.1109/PowerAfrica.2019.8928811.

[16] E. Zambolin and D. Del Col, "Experimental analysis of thermal performance of flat plate and evacuated tube olar collectors in stationary standard and daily conditions," Sol. Energy, vol. 84, no. 8, pp. 1382–1396, Aug. 2010, doi: 10.1016/j.solener.2010.04.030.

[17] J. A. Duffie and W. A. Beckman, "Solar radiation," in Solar Engineering of Thermal Processes, 4th ed. Hoboken, NJ, USA: John Wiley & Sons, 2013, ch. 1, pp. 3–42.

[18] Joint Committee for Guides in Metrology (JCGM), Evaluation of Measurement Data – Guide to the Expression of Uncertainty in Measurement (GUM), JCGM Standard 100:2008, 2008.

[19] [19] Tutiempo Network S.L. "Tutiempo Global Climate Data." en.tutiempo.net. tutiempo.net (accessed Mar. 7, 2025).

[20] G. L. Morrison, "Solar Collectors," in Handbook of Energy Efficiency and Renewable Energy, F. Kreith and D. Y. Goswami, Eds. Boca Raton, FL, USA: CRC Press, 2007, pp. 10-1–10-33.

[21] W. Wagner and A. Kruse, Properties of Water and Steam: The Industrial Standard IAPWS-IF97. Berlin, Germany: Springer, 1998.

[22] H. C. Hottel and A. Whillier, "Evaluation of flat-plate solar collector performance," in Trans. Conf. Use of Solar Energy: The Scientific Basis, Tucson, AZ, USA, 1958, vol. 2, part 1, pp. 74–104.

[23] D. C. Montgomery and G. C. Runger, Applied Statistics and Probability for Engineers, 7th ed. Hoboken, NJ, USA: John Wiley & Sons, 2018.

[24] World Health Organization, Legionella and the Prevention of Legionellosis, Geneva, Switzerland: WHO Press, 007.

[25] South African National Standards, Solar water heating systems Part 1: Domestic solar water heaters, SANS Standard 1307:2014, Ed. 5, 2014.

[26] American Society of Heating, Refrigerating and Air-Conditioning Engineers (ASHRAE), "Thermal insulation," in 2021 ASHRAE Handbook – Fundamentals, Atlanta, GA, USA: ASHRAE, 2021, ch. 26, pp. 26.1–26.21.

[27] National Energy Regulator of South Africa (NERSA), "Annual Report on Electricity Tariffs," Pretoria, South Africa, Tech. Rep., 2024.